Mass Spectrometric-Based Stable Isotopic 2-Aminobenzoic Acid Glycan Mapping for Rapid Glycan Screening of Biotherapeutics

Justin M. Prien,* Bradley D. Prater, Qiang Qin, and Steven L. Cockrill

Analytical Sciences, Amgen, Inc., 4000 Nelson Rd., Longmont, Colorado 80503

Fast, sensitive, robust methods for "high-level" glycan screening are necessary during various stages of a biotherapeutic product's lifecycle, including clone selection, process changes, and quality control for lot release testing. Traditional glycan screening involves chromatographic or electrophoretic separation-based methods, and, although reproducible, these methods can be time-consuming. Even ultrahigh-performance chromatographic and microfluidic integrated LC/MS systems, which work on the tens of minute time scale, become lengthy when hundreds of samples are to be analyzed. Comparatively, a direct infusion mass spectrometry (MS)-based glycan screening method acquires data on a millisecond time scale, exhibits exquisite sensitivity and reproducibility, and is amenable to automated peak annotation. In addition, characterization of glycan species via sequential mass spectrometry can be performed simultaneously. Here, we demonstrate a quantitative high-throughput MS-based mapping approach using stable isotope 2-aminobenzoic acid (2-AA) for rapid "high-level" glycan screening.

INTRODUCTION

Comprehensive glycan characterization is mandated for regulatory filing and biotherapeutic commercialization. However, at various stages of a biotherapeutic lifecycle, such as clone selection, quick "high-level" screening for specific glycan population distribution is more appropriate, rather than full characterization of the carbohydrate population. Traditionally, chromatographic or capillary electrophoretic (CE) separation-based methods perform these screening duties. However, with the advent of reducing end tags incorporating differential stable isotope labels, and the application of direct nanoelectrospray infusion, the rapid data acquisition rates and high throughput capabilities of mass spectrometry (MS) can be harnessed to provide a pairwise quantitative assessment of the glycan profile, in terms of glycan composition.

Various comparative labeling approaches for quantitative glycomics analysis have been reported in the literature.[1-10] These methods are analogous to the more-established approaches in the proteomics arena,[11-13] and they provide exquisite sensitivity, rapid data acquisition, and fundamental physical measurement-based analysis, thereby becoming an attractive alternative to physical separation-based quantitative approaches. Typically, reductive amination is used to introduce a fluorescent label to oligosaccharides, facilitating detection in the subsequent separation.[14,15] This routine chemistry may also be used to introduce various isotopic labeled substrates, such as $^{12}[C_6]$-aniline and $^{13}[C_6]$-aniline,[8,10] for pairwise MS-based comparison. Comparative online LC-MS analysis using blended samples relies upon the coelution of $^{12}[C_6]$- and $^{13}[C_6]$-labeled samples that do not drift like deuturated isotopic tags during chromatographic separation,[8,10,16,17] and the mass spectrometry-based detection of the associated mass difference of 6 Da between the $^{12}[C_6]$ and $^{13}[C_6]$ isotopic pair. Importantly, concerns regarding accurate MS-based relative quantitation are mitigated because of the presence of the internal isotopic labeled references, which exhibit almost-equivalent ionization efficiency, relative to their nonisotopic reciprocal. Recently, stable isotopic $^{12}[C_6]$−2-aminobenzoic acid ($^{12}[C_6]$−2-AA) and $^{13}[C_6]$−2-AA variants have become commercially available.

Certain factors must be considered when choosing the optimal reducing-end label, including label reactivity and compatibility with

* Author to whom correspondence should be addressed. Fax: (303) 401-4404. E-mail: justin.prien@amgen.com.

(1) Hitchcock, A. M.; Costello, C. E.; Zaia, J. *Biochemistry* **2006**, *45*, 2350–2361.
(2) Alvarez-Manilla, G.; Warren, N. L.; Abney, T.; Atwood, J., 3rd; Azadi, P.; York, W. S.; Pierce, M.; Orlando, R. *Glycobiology* **2007**, *17*, 677–687.
(3) Bowman, M. J.; Zaia, J. *Anal. Chem.* **2007**, *79*, 5777–5784.
(4) Kang, P.; Mechref, Y.; Kyselova, Z.; Goetz, J. A.; Novotny, M. V. *Anal. Chem.* **2007**, *79*, 6064–6073.
(5) Wada, Y.; Azadi, P.; Costello, C. E.; Dell, A.; Dwek, R. A.; Geyer, H.; Geyer, R.; Kakehi, K.; Karlsson, N. G.; Kato, K.; Kawasaki, N.; Khoo, K. H.; Kim, S.; Kondo, A.; Lattova, E.; Mechref, Y.; Miyoshi, E.; Nakamura, K.; Narimatsu, H.; Novotny, M. V.; Packer, N. H.; Perreault, H.; Peter-Katalinic, J.; Pohlentz, G.; Reinhold, V. N.; Rudd, P. M.; Suzuki, A.; Taniguchi, N. *Glycobiology* **2007**, *17*, 411–422.
(6) Hitchcock, A. M.; Yates, K. E.; Costello, C. E.; Zaia, J. *Proteomics* **2008**, *8*, 1384–1397.
(7) Kyselova, Z.; Mechref, Y.; Kang, P.; Goetz, J. A.; Dobrolecki, L. E.; Sledge, G. W.; Schnaper, L.; Hickey, R. J.; Malkas, L. H.; Novotny, M. V. *Clin. Chem.* **2008**, *54*, 1166–1175.
(8) Ridlova, G.; Mortimer, J. C.; Maslen, S. L.; Dupree, P.; Stephens, E. *Rapid Commun. Mass Spectrom.* **2008**, *22*, 2723–2730.
(9) Goetz, J. A.; Mechref, Y.; Kang, P.; Jeng, M. H.; Novotny, M. V. *Glycoconj. J.* **2009**, *26*, 117–131.
(10) Xia, B.; Feasley, C. L.; Sachdev, G. P.; Smith, D. F.; Cummings, R. D. *Anal. Biochem.* **2009**, *387*, 162–170.
(11) Gygi, S. P.; Rist, B.; Gerber, S. A.; Turecek, F.; Gelb, M. H.; Aebersold, R. *Nat. Biotechnol.* **1999**, *17*, 994–999.
(12) Aebersold, R.; Rist, B.; Gygi, S. P. *Ann. N.Y. Acad. Sci.* **2000**, *919*, 33–47.
(13) Griffin, T. J.; Gygi, S. P.; Rist, B.; Aebersold, R.; Loboda, A.; Jilkine, A.; Ens, W.; Standing, K. G. *Anal. Chem.* **2001**, *73*, 978–986.
(14) Anumula, K. R.; Dhume, S. T. *Glycobiology* **1998**, *8*, 685–694.
(15) Bigge, J. C.; Patel, T. P.; Bruce, J. A.; Goulding, P. N.; Charles, S. M.; Parekh, R. B. *Anal. Biochem.* **1995**, *230*, 229–238.
(16) Yuan, J.; Hashii, N.; Kawasaki, N.; Itoh, S.; Kawanishi, T.; Hayakawa, T. *J. Chromatogr., A* **2005**, *1067*, 145–152.
(17) Julka, S.; Regnier, F. *J. Proteome Res.* **2004**, *3*, 350–363.

additional chromatographic and mass spectrometric methods. For efficiency purposes, the same label should be utilized for all analytical aspects of a particular workflow, including rapid screening through detailed characterization. Beyond the availability of stable isotopic variants, 2-aminobenzoic acid (2-AA) confers many advantages over 2-aminobenzamide (2-AB), such as reactivity in aqueous derivatization conditions improving sample workflow efficiency and an increase in fluorescence intensity improving chromatographic sensitivity.[14,15,18] The 2-AA label affords an even greater advantage, with respect to mass spectrometric analysis, such as (1) improved ionization efficiency using positive-mode MALDI and negative-mode electrospray ionization (ESI), allowing enhanced detection of minor species;[19] (2) preferential reducing end deprotonation promoting efficient gas-phase glycan sequencing via sequential mass spectrometric (MS^n) disassembly from the nonreducing end to the reducing end of the glycomer;[20−23] (3) optimal compatibility with permethylation demonstrating a single intact mass species; and (4) availability of stable isotope analogs, as mentioned earlier.

Our current approach toward *de novo* glycan characterization employs a simple workflow devised around three core well-established analytical procedures: (1) 2-AA derivatization; (2) online reverse-phase separation coupled with negative-mode MS^n; and (3) permethylation derivatization with nanospray sequential mass spectrometry (NSI-MS^n) analysis. This workflow provides comprehensive *de novo* characterization of a biotherapeutic's glycan array, including structural isomers at ∼0.1% of the total chromatographic peak area. The focus of this manuscript is to describe a separation-free relative quantitation MS-based mapping approaching using 2-^{12}[C$_6$]AA and 2-^{13}[C$_6$]AA isotopically labeled substrates designed to meet our "high-level" high-throughput glycan screening needs via a logical ancillary extension of our multimethod workflow.

EXPERIMENTAL SECTION

Materials. Oligomannose-5 (M$_5$) standard from porcine thyroglobulin was purchased from Prozyme (San Leandro, CA). Proteomics-grade bovine ribonuclease B (RNase B), ^{12}[C$_6$]-aminobenzoic acid (2-^{12}[C$_6$]AA), ^{13}[C$_6$]-aminobenzoic acid (2-^{13}[C$_6$]AA), human blood serum IgG, and sodium hydroxide beads (small) were purchased from Sigma−Aldrich (St. Louis, MO). Normal-phase tips (DPS-6S resin, 10 μL bed volume) and Carbopack tips (40 μL bed volume) were sourced from PhyNexus Inc. (San Jose, CA). Macro SpinColumns were obtained from Harvard Apparatus (Holliston, MA). PNGase F was purchased from New England Biolabs (Ipswich, MA).

Enzymatic Release and Purification of RNase B N-glycans. *N*-linked glycans from 1 mg of bovine RNase B were released enzymatically, following slightly modified directions from the supplier. Protein and detergents were removed by a C$_{18}$ Sep-Pak,

and the flow-through fraction was desalted on porous graphitized carbon, as described below.[24] Purified glycans were dried via vacuum centrifugation.

Fluorescent Labeling. A 30 mg/mL solution of 2-^{12}[C$_6$]AA or 2-^{13}[C$_6$]AA were prepared in an acetate-borate-buffered methanol solution (4% sodium acetate trihydrate [w/v], 2% boric acid [w/v]). A 100-μL aliquot of 30 mg/mL 2-^{12}[C$_6$]AA or 2-^{13}[C$_6$]AA solution and 50 μL of 1 M sodium cyanoborohydride (NaBH$_3$CN) in tetrahydrofuran (THF) were added to enzymatic-released RNase B glycans or the M$_5$ standard, mixed and incubated at 80 °C for 1 h.

Sample Cleanup with Normal-Phase PhyTips. Excess ^{12}[C$_6$] and ^{13}[C$_6$] reducing-end label was removed from the reaction mixture using normal-phase DPA-6S PhyTips as described previously.[25] Briefly, PhyTips were prerinsed with 20% acetonitrile (ACN) and re-equilibrated with 96% ACN prior to loading of the diluted glycans. The excess label was removed by washing the loaded PhyTips four times with 96% ACN, and the glycans eluted with 20% ACN. Samples were dried via vacuum centrifugation and resuspended in 1 mL of HPLC-grade water.

Automated Porous Graphitized Carbon Desalting. PhyTip columns packed with a 40-μL porous graphitized carbon resin bed were supplied by PhyNexus (San Jose, CA). Resuspended samples were transferred to a 96-deep-well plate for desalting on the MEA system. Briefly, the PhyTips were prerinsed with 80% acetonitrile, 0.1% trifluoroacetic acid (TFA) and re-equilibrated with 100% HPLC-grade water prior to sample loading. The samples were washed three times with 100% HPLC-grade water, and the glycans were eluted with 25% ACN, 0.1% TFA. Samples were dried via vacuum centrifugation prior to analysis.

Solid-Phase Spin-Column Permethylation. Glycans were permethylated according to a previously reported method,[26] but slightly optimized for 2-AA derivatized species. Briefly, samples were resuspended in 60% dimethyl sulfoxide (DMSO), 37.2% iodomethane, and 2.8% water. To reduce the incidence of partial permethylation, 15 sample recycles, as opposed to 8 sample recycles for underivatized glycans, were employed. Note that reducing-end derivatized glycans tend to underpermethylate, compared to reduced and underivatized glycans. This can lead to some ambiguity with the interpretation of intact mass data acquired by direct infusion of complex biological glycan mixtures.

MALDI-TOF Mass Spectrometry. Matrix-assisted laser desorption ionization time-of-flight mass spectrometry (MALDI-TOF MS) analysis was performed using an Applied Biosystems 4800 Proteomics analyzer (Applied Biosystems, Framingham, MA) that was equipped with a 355-nm Nd:YAG laser. MALDI spectra were acquired in the positive mode. Dried labeled samples were reconstituted in 1:1 methanol:water. A quantity of 0.5 μL of reconstituted sample was mixed with 0.5 μL of 2,5-dihydroxybenzoic acid (DHB) matrix (12 mg/mL in 50% ACN (v/v) aqueous solution) and spotted onto a stainless steel MALDI target. Samples were ablated with a power of 3500 while the laser rastered over the target surface, accumulating 1000 profiles per sample spot.

(18) Anumula, K. R. *Anal. Biochem.* **2006**, *350*, 1–23.
(19) Pabst, M.; Kolarich, D.; Poltl, G.; Dalik, T.; Lubec, G.; Hofinger, A.; Altmann, F. *Anal. Biochem.* **2009**, *384*, 263–273.
(20) Chen, X.; Flynn, G. C. *Anal. Biochem.* **2007**, *370*, 147–161.
(21) Brull, L. P.; Kovacik, V.; Thomas-Oates, J. E.; Heerma, W.; Haverkamp, J. *Rapid Commun. Mass Spectrom.* **1998**, *12*, 1520–1532.
(22) Franz, A. H.; Lebrilla, C. B. *J. Am. Soc. Mass Spectrom.* **2002**, *13*, 325–337.
(23) Harvey, D. J.; Royle, L.; Radcliffe, C. M.; Rudd, P. M.; Dwek, R. A. *Anal. Biochem.* **2008**, *376*, 44–60.

(24) Hanneman, A. J.; Rosa, J. C.; Ashline, D.; Reinhold, V. N. *Glycobiology* **2006**, *16*, 874–890.
(25) Prater, B. D.; Anumula, K. R.; Hutchins, J. T. *Anal. Biochem.* **2007**, *369*, 202–209.
(26) Kang, P.; Mechref, Y.; Novotny, M. V. *Rapid Commun. Mass Spectrom.* **2008**, *22*, 721–734.

MS data processing was performed by DataExplorer 4.0 (Applied Biosystems).

Rapid Resolution Reverse-Phase HPLC. *N*-linked glycans released from 1 mg of RNase B were separated on an Agilent Zorbax Rapid Resolution SB-C18 column (2.1 mm × 50 mm, 1.8 μm) that was connected to an Agilent 1100 HPLC equipped with online fluorescence detection. The excitation and emission wavelength parameters were 360 and 425 nm, respectively. The mobile phases used were as follows: (A) 0.1% acetic acid (HOAc); (B) 5% ACN, 0.1% HOAc; and (C) 80% ACN, 0.1% HOAc. The system was operated at a constant flow rate of 333 μL/min with a column temperature of 50 °C. Following injection, reagents were eluted with a 2 min isocratic elution at 30% mobile phase B. This was followed by an initial gradient step of increasing mobile phase B at a rate of 0.55% per minute over 40 min, and then a second gradient step of increasing mobile phase B of 1.43% per minute over 7 min. Finally, the column was regenerated with 100% mobile phase C for 4 min and re-equilibrated under initial conditions for an additional 4 min prior to subsequent injection.

Online Negative-Mode Electrospray Mass Spectrometry (ESI-MS/MSⁿ). The outlet of the chromatographic separation was coupled directly to a linear ion trap mass spectrometer (Thermo LTQ XL, San Jose, CA) equipped with an electrospray ionization source. The instrument was tuned for 2-AA-labeled samples via the infusion of a 1 pmol/μL solution of the corresponding $^{12}[C_6]$AA-labeled oligomannose-5 standard in mobile phase A. The tuning solution was infused at 30 μL/min into a 30% mobile phase B background flow of 300 μL/min. The capillary temperature was set at 200 °C, and the spray voltage was −3.2 kV. For tandem MS/MS, parent ions were selected with an isolation window width of 5 m/z, the normalized collision energy was set at 35%, and the activation was conducted at $Q = 0.25$ for 50 ms. For subsequent MSⁿ stages, the isolation width window was set at 2 m/z, the collision-induced dissociation set at 35% with an activation $Q = 0.25$ for 50 ms. A wide m/z isolation width was utilized to isolate the entire isotopic envelope of each species, and this provides higher-quality spectral data at the later MSⁿ stages. Note that, with this approach, isobaric, isomeric, and nonisobaric species may be simultaneously isolated and subjected to subsequent MSⁿ disassembly.

Nanospray Mass Spectrometry (NSI-MS). Negative- and positive-mode mass spectrometric data of directly infused sample mixtures was obtained on a linear ion trap mass spectrometer (Thermo LTQ XL, San Jose, CA) equipped with a TriVersa Nanomate-automated nanospray ion source (Advion, Ithaca, NY). Signal averaging was accomplished by adjusting the number of scans, relative to the ion signal strength. For tandem MS/MS data acquisition, the isolation window width was set at 1.0 m/z. Collision parameters were left at default values with normalized collision energy set to 35%, or optimized to values leaving a minimal parent ion peak. Activation was set at a value of $Q = 0.25$ and an activation time of 30 ms.

RESULTS AND DISCUSSION

Figure 1 illustrates a straightforward experimental workflow for comparative glycan mapping of upward of 384 paired samples within ∼3 h. The development of this high-throughput workflow is based on three core features: (1) the availability of 2-AA as $^{12}[C_6]$ and $^{13}[C_6]$ stable isotopic variants; (2) adaptation of manual glycan purification procedures to a robotic automated purification platform; and (3) separation-free relative quantitative stable isotope MS-based analysis via direct infusion, which obviates lengthy chromatographic separation times. Briefly, equimolar amounts of protein are separately released enzymatically and differentially labeled in parallel with either the $^{12}[C_6]$ or $^{13}[C_6]$ fluorescent tag. Alternatively, for "absolute" quantitation, exact molar amounts of $^{13}[C_6]$-labeled glycan standards may be used. The differentially labeled samples are then blended in equal proportions during an automated clean-up step to remove excess label on a PhyNexus MEA purification system. The mixed sample undergoes a subsequent desalting via an automated porous graphitized carbon step using the same robotic platform. The equimolar differentially labeled paired sample is then subjected to MS-based relative quantitative analysis.

Relative Quantitation of 2-$^{12}[C_6]$AA and 2-$^{13}[C_6]$AA Labeled Glycan Standards. Various molar ratios (1:1; 2:1; 5:1; 10:1) of $^{12}[C_6]$- and $^{13}[C_6]$-labeled oligomannose-5 standard (M_5) derived from porcine thyroglobulin were used to determine the feasibility and dynamic range of a separation-free relative quantitation MS-based approach. Five replicates of each individual molar ratio (1:1; 2:1; 5:1; 10:1) were analyzed by both positive-mode MALDI-TOF MS and negative-mode NSI-MS. Figures 2a−d represent MALDI-TOF MS spectra of the M_5 standard ratios (1:1; 2:1; 5:1; 10:1). The parent ions, m/z 1379.04 and m/z 1385.06, represent intact sodium-adducted M_5-2-$^{12}[C_6]$AA and M_5-2-$^{13}[C_6]$AA species, respectively. As expected, the $^{13}[C_6]$-labeled species exhibits a mass offset of +6 Da. Importantly, the isotopic mass difference provides sufficient m/z value dispersion, so each isotopically labeled species may be distinguished and quantified without interference from the isotopic distribution of its differentially labeled counterpart. As the spectra (see Figures 2a−d) demonstrate, the ratios of M_5−2-$^{12}[C_6]$AA to M_5−2-$^{13}[C_6]$AA corresponds closely to the expected theoretical molar ratios (1:1; 2:1; 5:1; 10:1). The ratio of $^{13}[C_6]/^{12}[C_6]$ was calculated from the sum of the individual isotope intensities from each of the $^{13}[C_6]$- and $^{12}[C_6]$-labeled M_5 species. It was previously demonstrated that, when the monoisotopic peak intensity is used as a ratio indicator, the ratio value broadens as the glycomer increases in size.[2] As such, the ratios of $^{12}[C_6]$ to $^{13}[C_6]$ were calculated based on the sum of the intensities of the complete isotope peak distribution in this report. To determine the linearity and reproducibility of the method, five independent molar ratio sets of the M_5 standard were analyzed and the resultant M_5 calibration curve demonstrates linearity ($R = 0.9982$) between the expected and theoretical ratio values (see Figure S1a in the Supporting Information). More-dilute ratios (15:1; 20:1; and 50:1) of the differently labeled M_5 standard were utilized for limit-of-detection and edge-of-dynamic-range determination. Although the minor analog of the 20:1 sample pair was detectable, confident quantitation was unattainable (data not shown) and, therefore, suggests a 10-fold working range where confident quantitative results may be obtained. Given that this analysis is most likely to be performed in a manner relative to a similar glycan distribution, this is not considered to be a significant limitation of the method, unless samples of very different glycan populations are compared. However, note that the relative quantitation of low-abundance species pairs (e.g., M_9 in Figure 2e) does demonstrate reliable quantitation at or below 2% of the total glycan
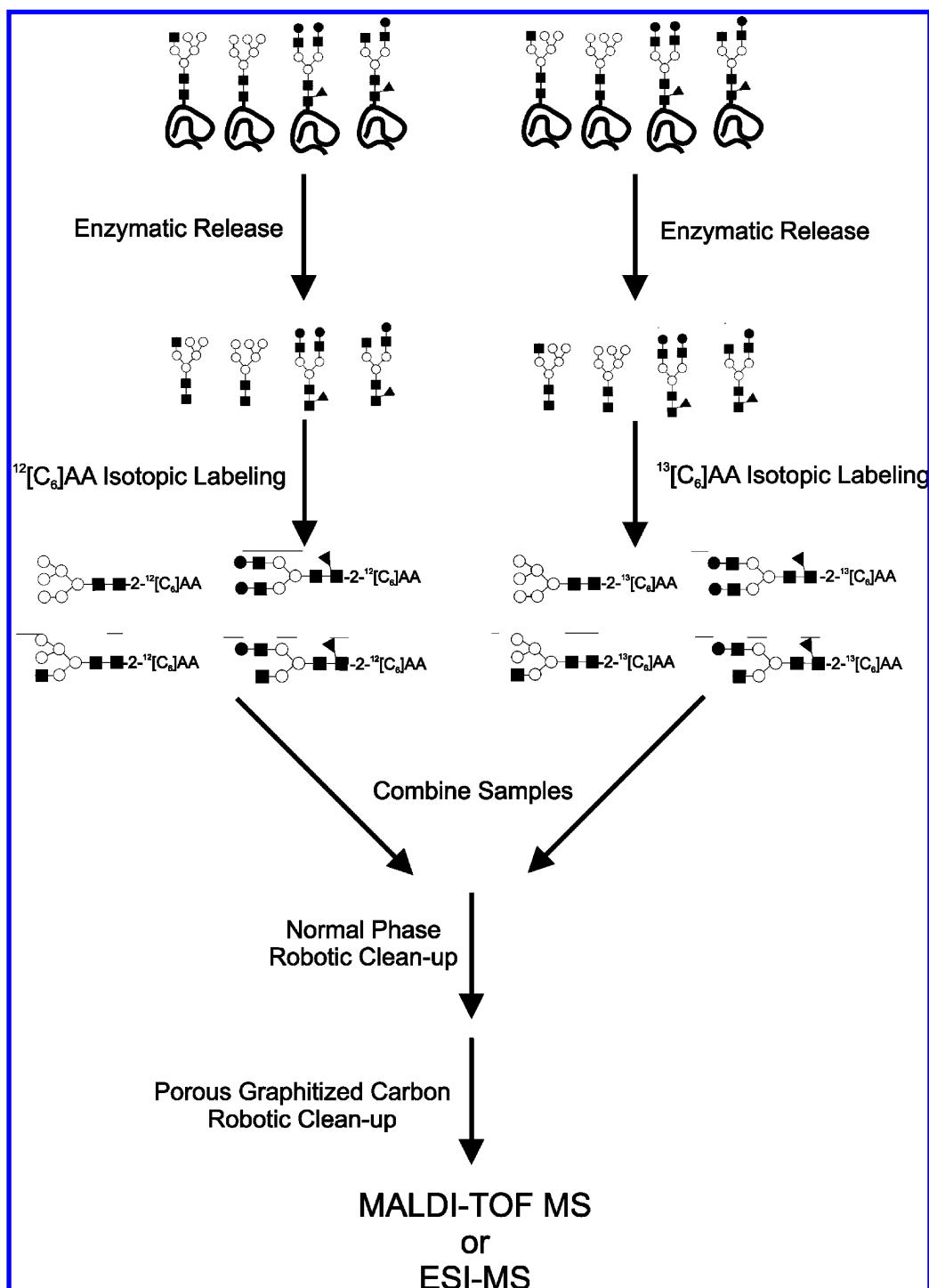
Figure 1. Stable isotope sample preparation workflow.

population (i.e., relative to the base peak). Although a rationale for this observation has yet to be postulated, these findings are consistent with previous reports using stable isotopic variants.[10] The base peak for these experiments represents a 7.4 pmol concentration of the labeled standard. As such, the limit of detection for positive-mode MALDI-TOF MS relative quantitative analysis is ~0.5 pmol for the M_5 species.

Equimolar aliquots of RNase B were simultaneously released and differentially labeled, according to the sample workflow outlined in Figure 1. Figure 2e depicts the positive-mode MALDI-TOF MS spectrum of a 1:1 mixture of $^{12}[C_6]$- and $^{13}[C_6]$-labeled glycans from RNase B. Immediately evident in the spectrum are six sets of doublets (1378.80/1384.89, 1540.99/1547.01, 1703.08/1709.10, 1744.10/1750.12, 1865.18/1871.20, and 2033.30/2027.28), which represent five sodium-adducted high-mannose species (M_5, M_6, M_7, M_8, and M_9, respectively) and one hybrid-type glycomer. The lower-abundance ion doublets satellite to the prominent sodiated species correspond to protonated as well as potassium-adducted iterations of the respective differentially labeled glycomers. Alkali-metal adduct formation is a common occurrence when MALDI-MS methodology is used for glycan analysis. Sodium acetate is often added to drive the adduct formation toward
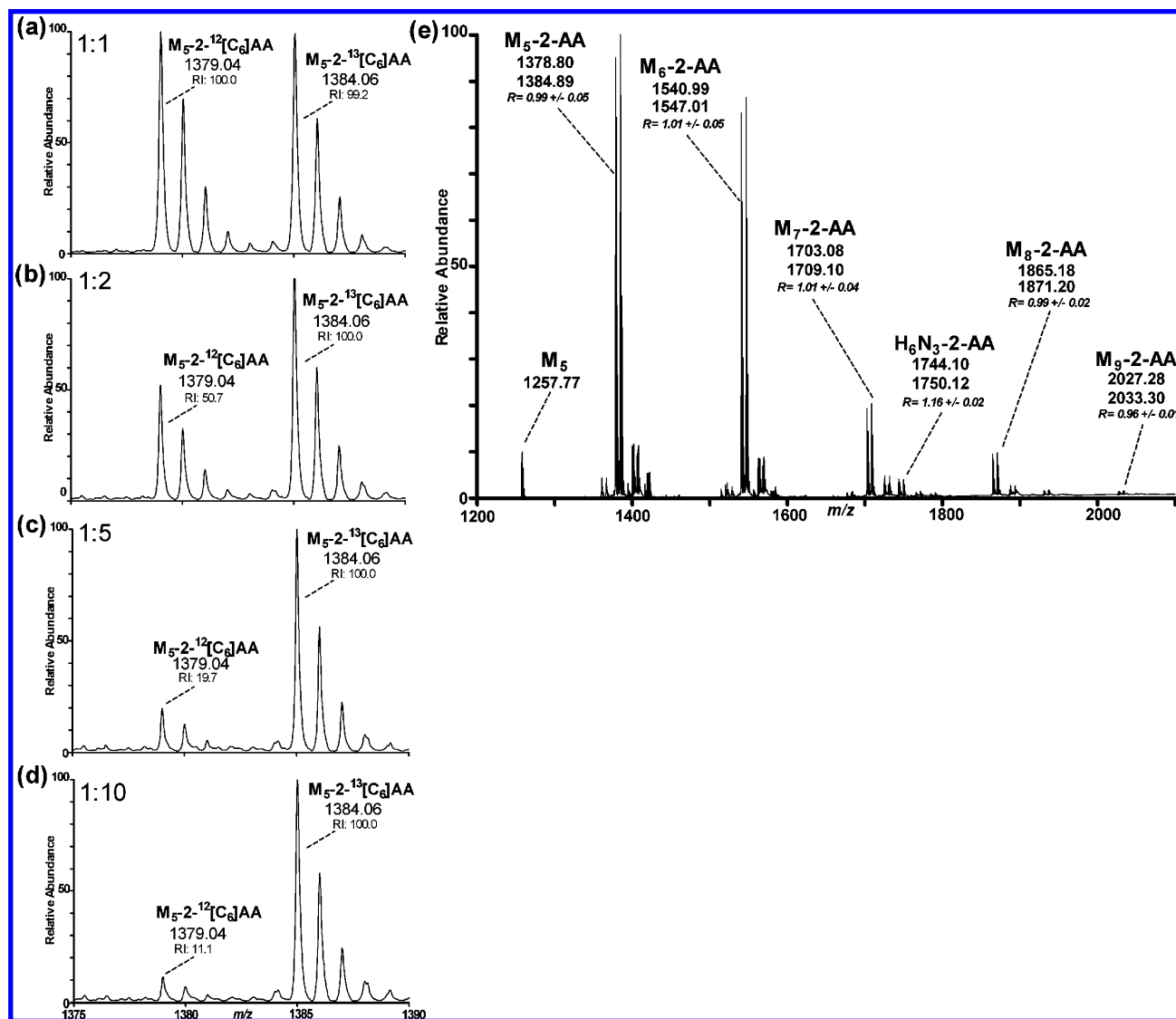
Figure 2. MALDI-TOF MS spectra representing various $^{12}[C_6]$:$^{13}[C_6]$ molar ratios of M_5 standard derived from porcine thyroglobulin: (a) 1:1, (b) 1:2, (c) 1:5, and (d) 1:10. (e) MALDI-TOF MS spectrum of a 1:1 ratio of enzymatically released glycans from bovine RNase B.

the desired sodium-adducted species.[27−29] The average ratio of the six sodium-adducted isotopic pairs calculated from five independent sample preparations was 1.02 (CV = 1.16%), which is consistent with the expected ratio of 1.0, signifying the accuracy and reproducibility of stable isotopic MALDI-TOF MS-based mapping for the relative quantitation of analogous glycan species. This is unsurprising, knowing that similar results were reported in an extensive HUPO multi-institutional study, which established MS-based quantitation correlative to established chromatographic methodologies.[5] In addition, many other studies detailing alternative MS quantitative glycomics approaches have reported similar results.[2,5,8,10]

Direct Nanospray Infusion of a 1:1 Mixture of 2-$^{12}[C_6]$AA- and 2-$^{13}[C_6]$AA-Labeled M_5 Standard Derived from Porcine

(27) Harvey, D. J.; Mattu, T. S.; Wormald, M. R.; Royle, L.; Dwek, R. A.; Rudd, P. M. *Anal. Chem.* **2002**, *74*, 734–740.

(28) Kang, P.; Mechref, Y.; Klouckova, I.; Novotny, M. V. *Rapid Commun. Mass Spectrom.* **2005**, *19*, 3421–3428.

(29) Mechref, Y.; Novotny, M. V.; Krishnan, C. *Anal. Chem.* **2003**, *75*, 4895–4903.

Thyroglobulin. The same five M_5 standard molar ratio sets (1:1; 2:1; 5:1; 10:1) used to assess the capabilities of MALDI-TOF MS for relative quantitation were also subjected to direct nanospray infusion ion trap mass spectrometry (NSI-MS) to evaluate whether relative quantitation of $^{12}[C_6]$- and $^{13}[C_6]$-labeled species may be performed in the negative mode. Similar to positive-mode MALDI-TOF MS, negative-mode NSI-MS demonstrates excellent linearity (R = 0.9992) and good reproducibility (see Figure S1b in the Supporting Information). Although the spectra for the entire ratio series are not presented, Figure 3a showcases the negative-mode NSI-MS spectrum of the 1:1 $^{12}[C_6]$-to-$^{13}[C_6]$ M_5 sample. This spectrum exhibits intact mass ions, m/z 1354.6 and m/z 1360.6, which is consistent with deprotonated M_5−2-$^{12}[C_6]$AA and M_5−2-$^{13}[C_6]$AA species, respectively; in a 1:1 ratio, which aligns with the expected ratio values, suggesting that negative-mode NSI-MS provides reproducible relative quantitative results within a 10-fold working range.

A significant disadvantage of MALDI-TOF analysis is the harsher ionization conditions that are experienced by analytes,
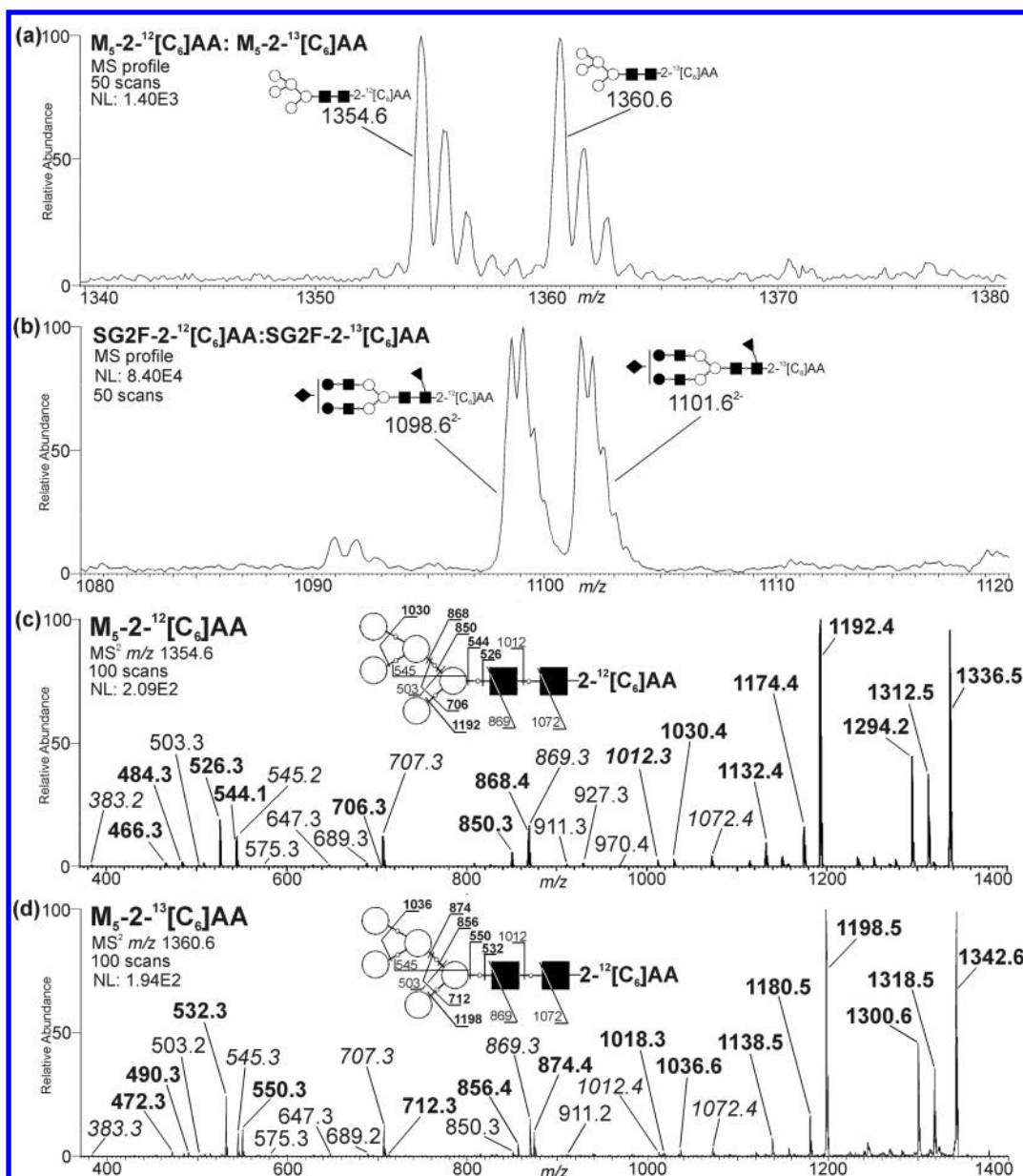
Figure 3. (a) Negative-mode NSI-MS spectrum of a 1:1 mixture of M_5 standard derived from porcine thyroglobulin. (b) Zoomed spectral view of NeuAc_1Hex_5HexNAc_4Fuc_1 composition 1:1 mixture of human IgG acquired via negative-mode NSI-MS. (c) Negative-mode tandem MS/MS spectrum of 2-^{12}[C_6]AA-labeled M_5 standard derived from porcine thyroglobulin. (d) Negative-mode tandem MS/MS spectrum of 2-^{13}[C_6]AA-labeled M_5 standard derived from porcine thyroglobulin.

which may result in undesirable cleavage of labile bonds. This phenomenon has been observed in disulfide-linked peptides[30,31] as well as glycans, particularly sialylated species,[2,4,9,26,28,32] and consequently renders quantitative analysis difficult. Alternatively, softer electrospray ionization conditions and operation in the negative mode are amenable to sialylated glycan analysis and has proven to be quite beneficial.[23,33−35] Equimolar aliquots of human IgG were simultaneously released and differentially labeled

according to the sample workflow outlined in Figure 1. Figure 3b depicts a zoomed view, focused on the NeuAc_1Hex_5HexNAc_4Fuc_1 composition, of a the negative-mode NSI-MS spectrum of a 1:1 mixture of the ^{12}[C_6]- and ^{13}[C_6]-labeled glycan pool from human IgG. The differentially labeled NeuAc_1Hex_5HexNAc_4Fuc_1 species is doubly deprotonated and the ^{13}[C_6]-labeled species exhibits the expected +3 m/z shift (see Figure 3b). Importantly, the isotopic mass difference provides sufficient m/z value dispersion, so each doubly charged isotopically labeled species may be distinguished and quantified without interference from its differentially labeled analog. The average ratio of six doubly charged doublets (m/z 1098.6/1101.6, 1244.6/1247.6, 1345.7/1348.7, 1171.1/1174.1, 1272.7/1275.7, and 1225.6/1228.6, corresponding to the sialylated compositions NeuAc_1Hex_5HexNAc_4Fuc_1, NeuAc_2Hex_5HexNAc_4Fuc_1, NeuAc_2Hex_5HexNAc_5Fuc_1, NeuAc_1Hex_5HexNAc_4, NeuAc_2Hex_5-

(30) Patterson, S. D.; Katta, V. *Anal. Chem.* **1994**, *66*, 3727–3732.
(31) Qiu, X.; Cui, M.; Li, H.; Liu, Z.; Liu, S. *Rapid Commun. Mass Spectrom.* **2007**, *21*, 3520–3525.
(32) Domon, B.; Costello, C. E. *Biochemistry* **1988**, *27*, 1534–1543.
(33) Harvey, D. J. *J. Am. Soc. Mass Spectrom.* **2005**, *16*, 647–659.
(34) Karlsson, N. G.; Schulz, B. L.; Packer, N. H. *J. Am. Soc. Mass Spectrom.* **2004**, *15*, 659–672.
(35) Karlsson, N. G.; Wilson, N. L.; Wirth, H. J.; Dawes, P.; Joshi, H.; Packer, N. H. *Rapid Commun. Mass Spectrom.* **2004**, *18*, 2282–2292.

HexNAc$_4$, NeuAc$_2$Hex$_5$HexNAc$_5$, respectively) from five independent preparations of the human IgG sample was calculated as 1.04 (CV = 3.74%) and demonstrates that negative-mode NSI-MS analysis is a suitable robust method for the relative quantitation of doubly charged analogous sialylated species between glycoprotein samples.

The various glycan classes (high-mannose, sialylated, sulfated, etc.), when analyzed in their native form, ionize with different efficiencies. For example, sialylated glycans ionize more readily than neutral glycans in the negative mode. As such, stable isotopic mapping of native glycans is a powerful method for relative quantitation of differentially labeled pairs, or even within a series of glycan species; however, it should not be used for "interspecies" quantitation.

Permethyl derivatization stabilizes sialic acid moieties and consequently neutralizes variation in ionization between neutral and sialylated glycan classes. These attributes allow for simultaneous quantitative analysis of neutral and sialylated glycan mixtures in the same MS spectrum.[2,4,9,26,28,32] Innovative methods for the relative quantitative analysis of permethylated glycans, such as differential permethylation using stable isotopic ^{12}[C] and ^{13}[C] methyl iodide variants, as well as deuteriopermethylation, have been developed.[2,4] A minor shortcoming of these methods is the that fact that the relative mass shift between isotopic pairs fluctuates, depending on the number of intrinsic hydroxyl groups (−OH) of the glycomer. That is, as the glycomers increase in regard to monosaccharide count, the mass shift between the isotopic pair increases. Contrastingly, stable isotopic reducing end labels provide 1:1 stoichiometry and a constant mass separation between the constituents of each isotopic pair, regardless of glycomer size.[8,10] An attractive alternative to stable isotopic permethyl derivatization for the relative quantitation of mixed glycan populations might be the combination of reducing end stable isotopic labeling and ^{12}[C$_6$] permethylation. With this combinatorial approach, neutral and sialylated glycan classes may be easily identified and quantitated in the same profile. In addition, if an ion trap instrument is used, subsequent *de novo* characterization via NSI-MS^n may be seamlessly performed on the directly infused unseparated differently labeled mixture.

Negative-Mode NSI-MS/MS Analysis of 2-^{12}[C$_6$]AA and 2-^{13}[C$_6$]AA Labeled M$_5$ Standard from Porcine Thyroglobulin. Under low-energy CID negative-mode conditions, multiple independent cleavage events occur, stimulating isobaric, "isobaric-like", and isomeric product ion formation. These ion types can originate from different regions of a single structure or stem from multiple structural isomers that are simultaneously present. As a result of this immense structural overlap, spectral interpretation and fragment ion structural assignment is a daunting task.[21−23,36,37] The introduction of a stable isotopic tag is an efficient way to alleviate isomeric complexity. The ^{13}[C$_6$] variant imparts a 6 Da mass shift, allowing segregation of reducing end fragment ions from their nonreducing end isomeric counterparts. Figures 3c and 3d represent the MS/MS spectra, *m/z* 1354.7 and *m/z* 1360.5, of a 1:1 mixture of ^{12}[C$_6$]- and ^{13}[C$_6$]-labeled M$_5$ standard derived from porcine thyroglobulin, respectively. A series of sequential neutral hexose losses (−162 Da), beginning with a ^{2,4}A$_4$ cross-

ring fragment, is observed in Figures 3c and 3d: *m/z* 869.3 → *m/z* 707.3 → *m/z* 545.2 → *m/z* 383.2. In Figure 3c, reducing end Y-ion fragments, *m/z* 868.4 (Y$_{3\alpha}$-ion), 706.3 (Y$_3$-ion), and 544.1 (Y$_2$-ion) are within one mass unit of the nonreducing end ^{2,4}A series ions. Without high-resolution and high-mass-accuracy instrumentation, differentiation and structural assignment of isobaric fragments can be difficult. Via the incorporation of a ^{13}[C$_6$] label, the nonreducing Y-ion fragments (Y$_{3\alpha}$, Y$_3$, and Y$_2$ ions) (highlighted in bold in Figure 3d) are appropriately shifted by +6 Da, compared to their corresponding ion in the ^{12}[C$_6$]-labeled sample (highlighted in bold in Figure 4c). This calculated displacement allows sufficient segregation of the once-isobaric fragment ions, thereby reducing spectral complexity and providing greater confidence in structural fragment ion assignment.

**Rapid Resolution Reverse-Phase Separation of High-Mannose and Hybrid-Type Glycan from Bovine RNase B.** Three 2-AA-derivatized glycan samples were used to assess whether or not ^{12}[C$_6$]- and ^{13}[C$_6$]-labeled glycans suffer from dispersion during chromatographic experimentation: (1) ^{12}[C$_6$]-labeled glycans derived from RNase B; (2) a 1:1 sample mixture of ^{13}[C$_6$]- and ^{12}[C$_6$]-labeled glycans from RNase B; and (3) a sample mixture of ^{12}[C$_6$]-labeled glycans from RNase B "spiked" with 7.4 pmol of ^{13}[C$_6$]-labeled M$_5$ standard from porcine thyroglobulin. Figure 4 depicts the reverse-phase chromatographic profiles of three 2-AA-derivatized glycan samples. The profiles of the ^{12}[C$_6$]-derivatized glycans from RNase B and the 1:1 mixture of ^{12}[C$_6$]- and ^{13}[C$_6$]-derivatized glycans from RNase B are indistinguishable, confirming that the stable isotope variants exhibit identical chromatographic behavior. The blended sample of ^{12}[C$_6$]-labeled RNase B glycans and ^{13}[C$_6$]-labeled M$_5$ standard presents a slightly different profile. Peaks 1b, 3, 4, and 5 in Figure 4 appear relatively suppressed, which is consistent with the addition of supplemental amounts of M$_5$ standard introduced into the sample mixture. Equally unsurprising is the increased peak area of peaks 1a, 5b, and 7a in Figure 4, which represent the elution points of the various M$_5$ isomers.[38] These findings illustrate 2-AA-stable-isotope-labeled glycan analogs coelute during reverse-phase chromatography and do not exhibit chromatographic dispersion. Table 1 represents the high-mannose and hybrid-type glycans identified in bovine RNase B via RRRP chromatography, as shown in Figure 4. Structural isomer identification was confirmed by permethylated sequential mass spectrometry.

Figure 5a depicts a negative-mode composite MS spectrum (signal averaged over the entire chromatographic run (9.45−38.00 min)) of a 1:1 mixture of ^{12}[C$_6$]- and ^{13}[C$_6$]-derivatized glycans from RNase B. Five sets of doublets—representing deprotonated high-mannose glycan species M$_5$ (*m/z* 1354.6/1360.6), M$_6$ (1516.7/1522.7), M$_7$ (1678.7/1684.5), and M$_8$ (1840/1846.8), and a single hybrid-type glycomer (*m/z* 1792.1/1797.8)—are present and demonstrate a relative abundance similar to the distribution demonstrated in the MALDI-TOF MS spectrum for the unfractionated RNase B glycan pool (see Figure 2e). Note that the low-abundance M$_9$ glycomer was identified, but not sufficiently resolved from the baseline to appear in the profile. Similar to the peripheral ion doublets observed in the MALDI-TOF MS spectrum

(36) Harvey, D. J. *J. Am. Soc. Mass Spectrom.* **2005**, *16*, 631–646.

(37) Wuhrer, M.; Koeleman, C. A.; Hokke, C. H.; Deelder, A. M. *Rapid Commun. Mass Spectrom.* **2006**, *20*, 1747–1754.

(38) Prien, J. M.; Ashline, D. J.; Lapadula, A. J.; Zhang, H.; Reinhold, V. N. *J. Am. Soc. Mass Spectrom.* **2009**, *20*, 539–556.
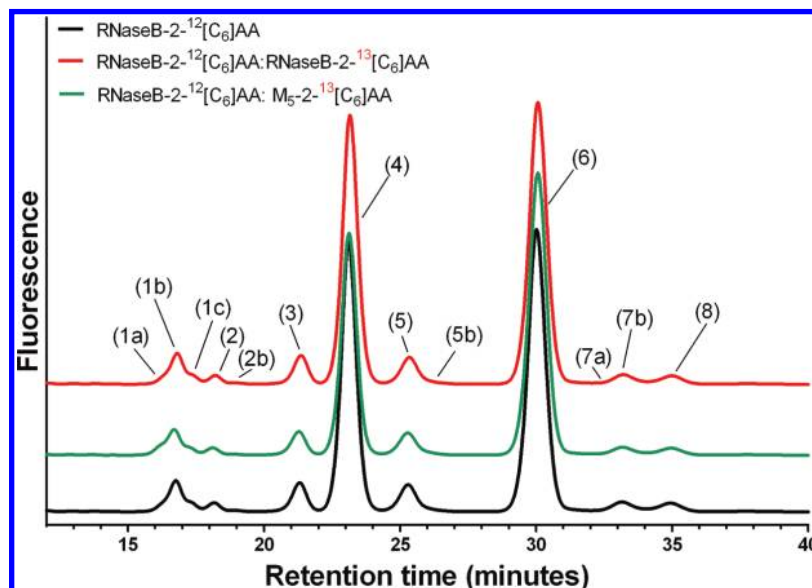
Figure 4. RRRP separation of stable isotopically labeled glycans from bovine RNaseB.

Table 1. Major Glycan Structures Identified in Bovine RNase B through RRRP Separation

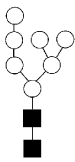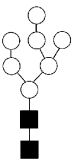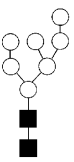| Peak	Composition	Observed mass/charge (*m/z*)	Theoretical mass (Da)	Structure
1a	H5N2	1354.50	1355.49	
1b	H8N2	1840.83	1841.75	
1c	H8N2	1840.83	1841.75	
2	M7N2	1678.75	1679.68	
2b	M8N2	1840.83	1841.75	
3	M7N2	1678.75	1679.68	
4	M6N2	1516.67	1517.62	
5	M7N2	1678.75	1679.68	
5b	M5N2	1354.5	1354.5	
6	M5N2	1354.5	1354.5	
7a	M5N2	1354.5	1354.5	
7b	M6N2	1516.67	1517.62	
8	H6N3	1719.75	1720.71	
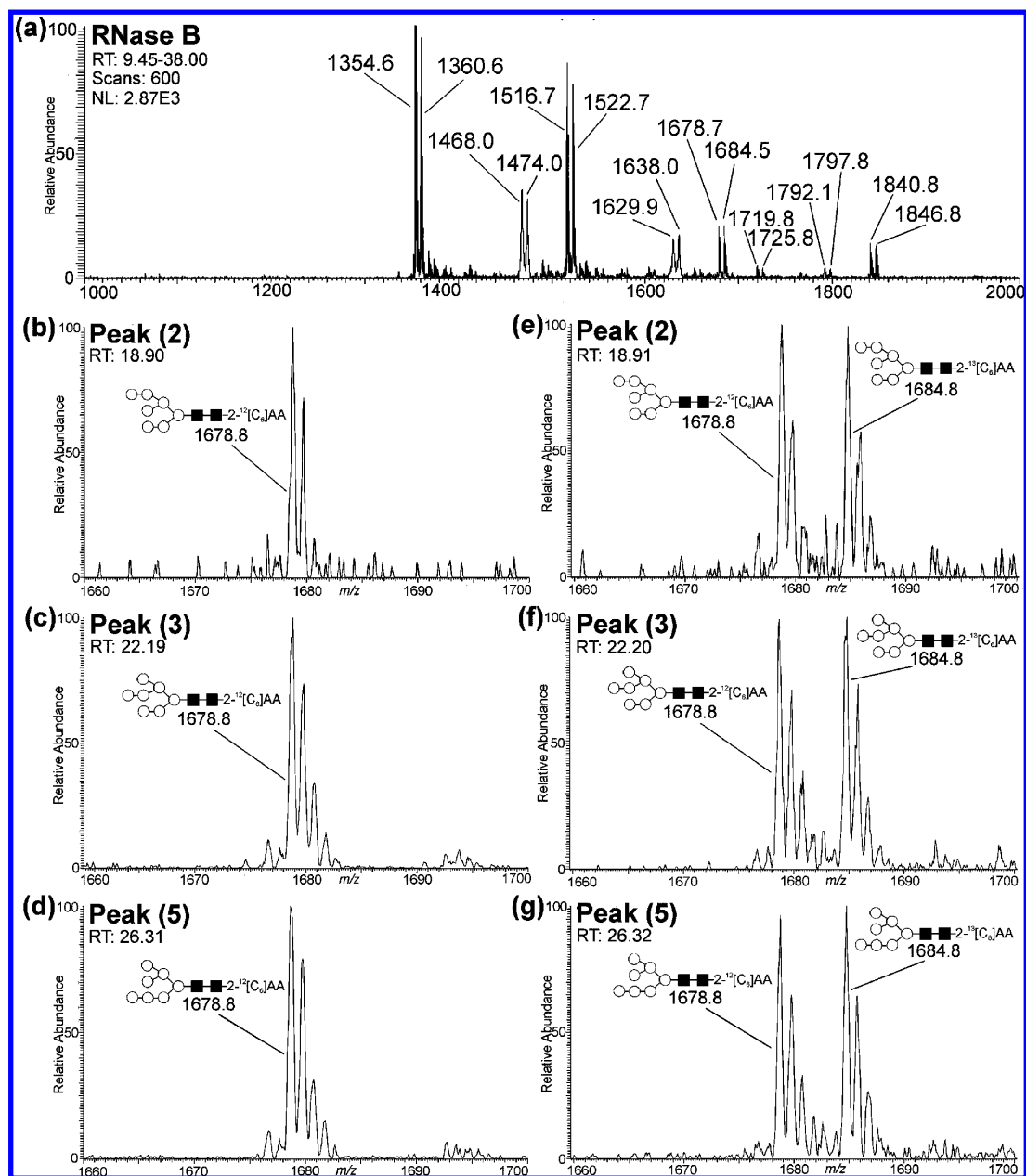
Figure 5. Online negative-mode NSI-MS spectra of various elution peaks from bovine RNase B: (a) composite MS spectrum signal average across the chromatograph run (9.45−38.00 min); (b) online RRRP negative-mode NSI-MS spectra of elution peak 2, from 2-^{12}[C$_6$]AA-labeled glycans from RNase B; (c) online RRRP negative-mode NSI-MS spectra of elution peak 3, from 2-^{12}[C$_6$]AA-labeled glycans from RNase B; (d) online RRRP negative-mode NSI-MS spectra of elution peak 5, from 2-^{12}[C$_6$]AA-labeled glycans from RNase B; (e) online RRRP negative-mode NSI-MS spectra of elution peak 2, from a 1:1 blended sample of 2-^{12}[C$_6$]AA- and 2-^{13}[C$_6$]AA-labeled glycans from RNase B; (f) online RRRP negative-mode NSI-MS spectra of elution peak 3, from a 1:1 blended sample of 2-^{12}[C$_6$]AA- and 2-^{13}[C$_6$]AA-labeled glycans from RNase B; and (g) online RRRP negative-mode NSI-MS spectra of elution peak 5, from a 1:1 blended sample of 2-^{12}[C$_6$]AA- and 2-^{13}[C$_6$]AA-labeled glycans from RNase B.

of RNase B (see Figure 2e), a triplet of doublets—m/z 1468.0/ 1474.0, 1629.9/1638.0, and 1792.1/1797.8—is present in the negative-mode composite spectrum (see Figure 5a). These ions represent double-acetate-adducted [M-3H + 2CH$_3$COOH]$^−$ iterations of the M$_5$, M$_6$, and M$_7$ glycomers, respectively. Most notably, the relative abundance of the high-mannose and hybrid-type glycans in the online negative-mode composite spectrum are correlative to the relative abundance of the analogous high-mannose and hybrid-type glycans that is depicted in the positive-mode MALDI-MS profile, as shown in Figure 2e.

Figures 5b−d depict the negative-mode MS profiles of peaks 2, 3, and 5 from the ^{12}[C$_6$]-labeled RNase B released glycan

sample. The parent ion m/z 1678.8 present in the MS profile from each peak is consistent with a Hex$_7$GlcNAc$_2$ composition and representative of the M$_7$ structural isomers. For M$_7$ structural isomer characterization, peaks 2, 3, and 5 were collected and subjected permethyl derivatization and subsequent NSI-MS^n analysis. The specific permethylated MS^n fragment ion pathways used to confidently assign structure are presented in Table 2. Figures 5e−g represents the MS profiles of peaks 2, 3, and 5 from a 1:1 mixture of ^{12}[C$_6$]- and ^{13}[C$_6$]-derivatized glycans derived from RNase B. The expected parent ion of the ^{13}[C$_6$]-labeled M$_7$ species has a mass offset of +6 Da, i.e., m/z 1684.8. As the spectra in

Table 2. Permethylated MS^n Pathways and Topologies for 2-^{12}[C$_6$]AA-Derivatized Sodium-Adducted Ion m/z 1080.1, Corresponding to the 2-AA-Labeled Composition Hex$_7$HexNAc$_2$ from Bovine RNase B

Putative Structures	M$_7$N$_2$-2-^{12}[C$_6$]AA		
	1	2	3
	Peak (5)	Peak (3)	Peak (2)
	(D1)	(D2)	(D3)

MS^n Pathways	Consistent Topologies
1080.1^{2+} → 1710.8 (loss of ■) → 1492.8 (loss of ○–) → 1288.6 (loss of –○–) → 1084.4 (loss of –○–) → 866.4 (loss of ○–) → 458 (○–■)	D1
1080.1^{2+} → 1710.8 (loss of ■) → 649.3 (○–○–○, B$_3$-type ion) → 547.3 (^{3,5}A ion) → 445.2 (○–○, B$_2$-type ion)	D1
1080.1^{2+} → 1710.8 (loss of ■) → 1492.8 (loss of ○–) → 1288.6 (loss of –○–) → 1084.4 (loss of –○–) → 866.4 (loss of ○–) → 648.2 (loss of ○–)	D1
1080.1^{2+} → 1710.8 (loss of ■) → 1492.8 (loss of ○–) → 1288.6 (loss of –○–) → 1070.5 (loss of ○–) → 866.4 (loss of –○–)	D1, D2, D3
1080.1^{2+} → 1710.8 (loss of ■) → 1492.8 (loss of ○–) → 1288.6 (loss of –○–) → 1070.5 (loss of ○–) → 880.4 (loss of ○–)	D2, D3
1080.1^{2+} → 1710.8 (loss of ■) → 871.4 (○–○/○–, or equiv., C$_4$-type ion) → 505.3 (^{0,4}A$_2$-ion) → 445.2 (○–○, B$_2$-type ion)	D3
1080.1^{2+} → 1710.8 (loss of ■) → 871.4 (○–○/○–, or equiv., C$_4$-type ion) → 533.3 (^{3,5}A$_2$-ion) → 445.2 (○–○, B$_2$-type ion)	D3
1080.1^{2+} → 1710.8 (loss of ■) → 871.4 (○–○/○–, or equiv., C$_4$-type ion) → 547.3 (^{3,5}A$_2$-ion) → 445.2 (○–○, B$_2$-type ion)	D2
1080.1^{2+} → 1710.8 (loss of ■) → 871.4 (○–○/○–, or equiv., C$_4$-type ion) → 563.4 (^{1,4}A$_2$-ion) → 463.2 (○–○–, C$_2$-type ion)	D2

Figures 5e−g demonstrate, the M$_7$ positional isomers (D3, D2, and D1, respectively) separate chromatographically, while the differentially labeled analogous M$_7$ isomers coelute. As such, online RRRP-(−)-mode MS/MS analysis of ^{12}[C$_6$] and ^{13}[C$_6$] differentially labeled samples is a powerful method for monitoring changes in the level of structural isomers between samples, should relative quantitation of isomeric groups be insufficient.

As the biopharmaceutical industry knows all too well; variation in high mannose content can have a dramatic effect on drug clearance and pharmacokinetic activity.[39−46] The availability of stable isotopic variants, superior chromatographic sensitivity, and higher-quality negative-mode mass spectral data of 2-AA-labeled glycans makes pairwise stable isotopic glycan mapping an attractive alternative to more-conventional 2-AB quantitative methods for drug clearance and human pharmacokinetic studies.[20,39] With the use of ^{12}[C$_6$] and ^{13}[C$_6$] stable isotopic fluorescent labeling, the differential clearance of high-mannose structural isomers may be monitored and quantitated in a pairwise manner. That is, a blended sample composed of enzymatically released glycans from isolated drug product that had been blood-drawn at a specific time point and released glycans from the preadministered drug product may be relatively quantitated in the same chromatographic run,

(39) Chen, X.; Liu, Y. D.; Flynn, G. C. *Glycobiology* **2009**, *19*, 240–249.

(40) Hotchkiss, A.; Refino, C. J.; Leonard, C. K.; O'Connor, J. V.; Crowley, C.; McCabe, J.; Tate, K.; Nakamura, G.; Powers, D.; Levinson, A.; et al. *Thromb. Haemostasis* **1988**, *60*, 255–261.

(41) Huang, L.; Biolsi, S.; Bales, K. R.; Kuchibhotla, U. *Anal. Biochem.* **2006**, *349*, 197–207.

(42) Jones, A. J.; Papac, D. I.; Chin, E. H.; Keck, R.; Baughman, S. A.; Lin, Y. S.; Kneer, J.; Battersby, J. E. *Glycobiology* **2007**, *17*, 529–540.

(43) Keck, R.; Nayak, N.; Lerner, L.; Raju, S.; Ma, S.; Schreitmueller, T.; Chamow, S.; Moorhouse, K.; Kotts, C.; Jones, A. *Biologicals* **2008**, *36*, 49–60.

(44) Stahl, P. D. *Curr. Opin. Immunol.* **1992**, *4*, 49–52.

(45) Stockert, R. J. *Physiol. Rev.* **1995**, *75*, 591–609.

(46) Sutton, C. W.; O'Neill, J. A.; Cottrell, J. S. *Anal. Biochem.* **1994**, *218*, 34–46.

CONCLUSION

During the development and commercialization of biotherapeutic molecules, the detection and detailed characterization of the drug's glycan array is a regulatory requirement. However, for certain operations, such a clone selection, process changes, and quality control, fast "high-level" high-throughput glycan population screening methods are more appropriate and satisfactory. With the advent of stable isotopic reducing end tags, and the application of direct nanoelectrospray infusion, the high-throughput capabilities of mass spectrometry (MS) can be exploited, providing rapid pairwise quantitative analysis of the glycan profiles (on the order of millisecond analytical time scales), thereby eliminating the need for lengthy separation-based screening methods. Here, we have introduced a reproducible high-throughput MS-based quantitative workflow that includes the incorporation of differentially labeled stable isotope labeled tags, robotic sample purification, and separation-free MS-based relative quantitation analysis, which can handle up to 384 individual paired samples within ~3 h. It is noteworthy that the majority of this analysis time is associated with the sample preparation, including enzymatic deglycosylation, labeling, and cleanup. Improvements in sample processing throughput were discussed in this report; however, further efficiencies could be gained through the utility of immobilized PNGase F and the development of rapid labeling chemistries.

Significant advantages are conferred by the simultaneous purification of multiple glycan samples in a parallel workflow over serial online workflow strategies. While novel integrated microfluidic workflows rapidly acquire glycan mapping data for individual samples, robotic sample workflows provide superior high-throughput capabilities when hundreds of samples are to be analyzed. For example, an online 10-min integrated workflow takes over 16 h to complete data acquisition for 100 individual samples, while a parallel robotic workflow at-line with MS-based relative quantitation takes ~3 h. In addition to the obvious time savings, reductions in consumable and disposal costs are also gained. These cost savings come from the elimination of expensive chromatographic columns and a complete reduction in acetonitrile use, as well as the associated removal of hazardous HPLC waste. As such, signification cost avoidances and time savings can be amassed through the implementation of a stable isotope MS-based quantitation methodology for all routine "high-level" high-throughput screening activities.

With the incorporation of recent developments toward the immobilization of deglycosylation enzymes and improved labeling chemistries, the notion of almost-instantaneous sample preparation and comparative MS-based glycan screening may soon be a reality.

SUPPORTING INFORMATION AVAILABLE

Depiction of the isotopically labeled M_5 standard derived from porcine thyroglobulin calibration curve. This material is available free of charge via the Internet at http://pubs.acs.org.